Submitted to the International Europhysics Conference on High Energy Physics,
HEP97, Jerusalem, Israel, August 1997

Observation of Events with a High Energy Isolated Lepton and Missing Transverse Momentum at HERA

H1 Collaboration

Abstract

At the HERA electron-proton collider a search for events with an imbalance in transverse momentum has been performed by H1. While the majority of events show topologies as expected for events of the charged current type ($e^+p \rightarrow \nu X$) five events have been observed with an isolated e^- or $\mu^\pm$ of high transverse momentum. Two of these events are found in a region of phase space as expected for the production of a W decaying leptonically.

Abstract 708
Parallel Sessions 7, 9, 11, 12, 13
Plenary Sessions 9, 15, 17

1 Introduction

In 1994 an event [1, 2] of unusual characteristics ($e^+p \to \mu^+ X$) was observed in the H1 detector at the HERA electron-proton storage ring. The event resulted from the standard charged current analysis [3]. The event exhibits an isolated high momentum muon recoiling against a system of hadrons. The event is unbalanced in transverse momentum suggesting the presence of an undetected final state particle. The event was recorded in an integrated luminosity of 3.2 pb^{-1}.

The present paper reports on a search for high energy isolated leptons in events which are unbalanced in transverse momentum. The data sample analyzed corresponds to an eightfold increase in luminosity.

2 Data analysis

2.1 Experimental conditions

This analysis is based on positron (27.6 GeV) - proton (820 GeV) collisions recorded by the H1 detector from 1994 to 1996 and part of 1997. It is restricted to periods with the H1 central tracker, liquid argon calorimeter and instrumented iron active and fully operational. The corresponding integrated luminosity is 24.7 ± 0.6 pb^{-1}.

A detailed description of the H1 detector can be found in [4].

A system of central and forward drift chambers (DC) is used to measure the charged particle trajectories and determine the interaction vertex. A magnetic field of 1.15 Tesla yields a measurement of the particle transverse momenta P_T with a nominal resolution $\sigma_{P_T}/P_T^2 = 3 \times 10^{-3}$ GeV^{-1}.

The hadronic and electromagnetic final state particles are absorbed in a highly segmented liquid argon (LAr) calorimeter [5], corresponding to between 5 and 8 interaction lengths depending on the emission angle of the particle. Electromagnetic shower energies are measured with a precision of $\sigma(E)/E = 12\%/\sqrt{E/\mathrm{GeV}}$ and hadronic shower energies with $\sigma(E)/E = 50\%/\sqrt{E/\mathrm{GeV}}$ applying an off-line weighting technique. The overall energy scales are known to 3% and 4% respectively.

The liquid argon calorimeter is surrounded by a superconducting coil and an iron yoke instrumented with streamer tubes. Leakage of hadronic showers outside the LAr calorimeter is measured from an analog sampling of the streamer tubes (Tail Catcher TC) with a resolution of $\sigma(E)/E = 100\%/\sqrt{E/\mathrm{GeV}}$. Penetrating charged particles like muons escaping the LAr calorimeter are tracked from their hit pattern in the streamer tubes with an efficiency greater than 90%.

The trigger condition for high transverse energy interactions is based on LAr signals. The trigger efficiency is higher than 95% for events with a scattered electron above 10 GeV, and higher than 85% for events with a missing transverse momentum greater than 25 GeV.

2.2 Event selection

The analysis adopts the framework of charged current (CC) studies [3] in order to identify interactions with a significant missing transverse momentum. The basic requirement is a calorimetric missing transverse momentum P_T^{calo} greater than 25 GeV. P_T^{calo} is defined as the transverse component of the vectorial sum of all energy deposits recorded in the LAr and TC calorimeters. In addition beam-gas background is rejected by requiring a reconstructed vertex in the interaction region, and most of non e–p interactions induced by cosmic and halo muons are removed using a set of topological and timing filters. A few remaining badly measured neutral current events with energy loss in the LAr calorimeter gaps, the tail-catcher or the beam-pipe are cut by excluding events with an identified scattered positron balancing the hadronic system in azimuth within 5°. After removal of residual non e–p background by visual scanning the final inclusive CC sample consists of 336 events.

The selection defined above is purely inclusive with respect to the presence of isolated charged leptons. The search for such final states is based on the presence of tracks with a polar angle greater than 10° and with transverse momenta higher than 10 GeV measured with an relative error smaller than 100%. The isolation of those high transverse momentum tracks is quantified from

- their distance D_{jet} to the closest hadronic jet in the pseudorapidity-azimuth plane $\eta - \phi$, defined by $D_{jet} = \sqrt{(\Delta\eta_{track-jet})^2 + (\Delta\phi_{track-jet})^2}$. Hadronic jets are identified with the cone algorithm ($R < 1$, $E_T > 5$ GeV) requiring in addition a jet transverse size in the (η,ϕ) plane larger than 0.1 and a jet energy electromagnetic fraction smaller than 0.9.
- their distance D_{track} to the closest DC track in $\eta - \phi$, defined in an analogous way. Here only well measured tracks with a polar angle greater than 5° are considered.

Figure 1a) shows the correlation between D_{track} and D_{jet} for all the high energy tracks in the CC inclusive sample. Five events are found with well isolated tracks.

LAr and instrumented iron signals associated with the tracks are used for lepton identification by demanding:

- electron case : A LAr electromagnetic shower with lateral and longitudinal shapes compatible with those expected from an electron or an positron has to match geometrically the track. The electron kinematical parameters are computed from the LAr shower.
- muon case : The track has to match geometrically a significant instrumented iron signal (muon system track or TC energy deposits). The muon kinematical parameters are computed from the DC track.

Figure 1b) shows the correlation between D_{track} and D_{jet} for the final CC sample with a lepton candidate as defined above.

In most of the cases the lepton candidates are located within or close to the CC hadronic shower. However five CC candidates show up with a lepton well isolated ($D_{jet} > 0.5$ and $D_{track} > 0.5$) from both other charged tracks and hadronic jets, and in a region well separated from the rest of the CC events.

After application of the CC selection and with the observation of isolated leptons in the resulting event sample, 331 events are identified without isolated leptons, 3 events contain an isolated muon, 1 event contains an isolated electron, and 1 event contains both an isolated positron and an isolated muon.

The five events containing isolated leptons are described in detail in the next section.

	ELECTRON	MUON-1	MUON-2	MUON-3	MUON-4
The isolated lepton :					
Charge (significance)	Neg.(5σ)	Pos.(5σ)	Pos.(5σ)	Neg.(5σ)	Neg.(2.7σ)
Transverse momentum (GeV)	$37.6^{+1.3}_{-1.3}$	$23.4^{+7.5}_{-5.5}$	$27.7^{+6.4}_{-4.4}$	$39.4^{+9.4}_{-6.4}$	$81.5^{+47.1}_{-21.9}$
Polar angle	$27.3 \pm 0.2°$	$46.2 \pm 1.3°$	$28.9 \pm 0.1°$	$35.2 \pm 0.1°$	$28.5 \pm 0.1°$
The hadronic system :					
P_T^X (GeV)	8.0 ± 0.8	42.2 ± 3.8	67.5 ± 5.4	27.5 ± 2.7	59.8 ± 5.9
$P_{\|\|}$ (GeV)	-7.2 ± 0.8	-42.1 ± 3.8	-61.9 ± 4.9	-12.5 ± 2.0	-57.4 ± 5.6
$P_{\perp}$(GeV)	-3.4 ± 0.9	-2.7 ± 1.8	26.8 ± 2.7	-24.5 ± 2.6	-16.6 ± 3.2
P_z (GeV)	79.9 ± 4.4	153.1 ± 9.1	247.3 ± 18.9	184.4 ± 13.2	118.0 ± 12.1
E (GeV)	81.1 ± 4.5	162.0 ± 10.0	257.1 ± 19.5	187.5 ± 13.6	140.8 ± 13.7
Mass (GeV)	11.8 ± 4.1	32.1 ± 9.2	20.4 ± 7.5	20.0 ± 12.7	48.4 ± 6.8
Global event properties :					
P_T^{miss} (GeV)	30.6 ± 1.5	$18.9^{+6.6}_{-8.3}$	$43.5^{+5.4}_{-6.4}$	$43.3^{+8.0}_{-5.3}$	$29.2^{+44.1}_{-13.4}$
$\delta = \sum E(1-\cos\theta)$(GeV)	10.4 ± 0.7	$18.9^{+3.9}_{-3.2}$	$17.0^{+1.9}_{-1.5}$	$27.7^{+3.4}_{-2.6}$	$43.6^{+12.2}_{-6.1}$
Transverse lepton-ν Mass (GeV)	67.7 ± 2.7	$3.0^{+1.5}_{-0.9}$	$22.6^{+5.0}_{-3.6}$	$77.8^{+18.0}_{-12.2}$	$93.2^{+100.0}_{-46.5}$

Table 1: Event kinematics : P_T^X measures the transverse momentum of the hadronic final state. $P_{||}$ and $P_{\perp}$ denote the hadronic transverse momenta components parallel and perpendicular to the transverse momentum of the isolated lepton, respectively.

2.3 Event kinematics

Displays of the five events are shown in figures 2 - 6. In each event an isolated track of high transverse momentum is recorded in the tracking system. This track is linked in one event (ELECTRON) to an electromagnetic cluster in the LAr calorimeter. In the other four events (MUONS) the isolated track is linked to small energy depositions in the LAr calorimeter and to a track observed in the instrumented iron system. In addition to the isolated track in all events a shower of hadronic origin is recorded in the LAr calorimeter correlated to tracks observed in the central and forward tracking system. In the following we give details of the events which are summarized quantitatively in table 1 .

The MUON events

The isolated track is measured in the central track detector, the liquid argon (LAr) calorimeter and in the muon chambers of the instrumented iron return yoke. The track as reconstructed in the tracking system is extrapolated through the calorimeter and the coil to the instrumented iron system. Taking into account the magnetic field traversed and the expected multiple scattering and energy loss in the material along the path, the track is linked to a track reconstructed in the muon chambers. The specific ionization dE/dx as measured in the DC is consistent with the interpretation that a single minimum ionizing track penetrates the chamber. Also the energy deposition in the liquid argon calorimeter is compatible with that expected from a minimum ionizing particle. The signals (hit multiplicity, energy deposition) recorded in the instrumented iron are as expected for a single penetrating particle.

In summary, the signals seen in the central track detector, the calorimeter and the instrumented iron system strongly support the interpretation of the isolated track as a muon. One event (MUON-3) shows the signature of an additional positron ($E = 7.7 \pm 0.4\,\mathrm{GeV}, \theta = 118.0 \pm 1.1°$)

The ELECTRON event

The event shows an isolated track measured in the central jet chamber (CJC) with a specific ionization compatible with a minimum ionizing particle. The track is linked to an energetic cluster (E=82 GeV, E_T=38 GeV) in the electromagnetic part of the calorimeter. The shower pattern is as expected for a shower of electromagnetic origin. The curvature measured for the track is compatible with a track of transverse momentum P_T=38 GeV with negative charge, whereas a positive charge is inconsistent at the level of 5 standard deviations.

The kinematic event balance

The momentum balance has been calculated from the lepton momentum and the total hadronic energy deposition (in event MUON-3 also the detected e^+ is taken into account).

In all events an imbalance in total transverse momentum $P_T^{miss} = |\vec{P}_T^{lepton(s)} + \vec{P}_T^X|$ is observed. The imbalance in the total transverse momentum is ascribed to unobserved particles carrying transverse momentum. In the events also a deficit is seen in the longitudinal direction, quantified by $\delta = \sum E(1 - \cos\theta)$, where E and θ denote the energy and polar-angle (measured with respect to the proton direction) of any detected particle. For an event where only longitudinal momentum along the proton direction (proton-remnant region) is undetected one would expect $\delta = 2E_e = 55\,\mathrm{GeV}$, with E_e being the energy of the incident positron. All events apart from MUON-4 show a significantly lower value of δ.

For the event MUON-4 the value of P_T^{miss} is compatible with zero within two standard deviations. However one observes a significant component $P_\perp$ of hadronic transverse momentum perpendicular to the transverse momentum of the muon. This fact supports the conclusion that particles carrying transverse momentum have escaped detection.

3 Discussion

Within the standard electroweak theory, the main processes expected to yield a sizeable rate of events with missing transverse momentum and a high P_T isolated lepton are those involving production and leptonic decay of a W boson. These processes are described first and then compared to the data. Alternative interpretations of the observed events are discussed afterwards.

3.1 *W* production

The cross-sections for W production and virtual exchange are quantitatively evaluated in [6] and were cross-checked independently [7].

The main contribution to the cross-section is due to photoproduction interactions with radiation of a real $W^\pm$ from the quark line, followed by its leptonic decay ($\mathrm{e}^+\mathrm{p} \rightarrow \mathrm{e}^+ WX, W \rightarrow \mathrm{e}^\pm\nu$ or $W \rightarrow \mu^\pm\nu$) with total cross section $\sim$ 70 fb per channel and charge. It is peaked at low values of the transverse momentum P_T^X of the recoil hadron system X, and shows a Jacobian peak at the W mass value in the lepton-neutrino transverse mass $M_T^{\ell\nu}$ spectrum. The scattered positron is observed in the main H1 detector in 25% of the cases. W^+'s and W^-'s are produced with similar rates.

About 10 % of the cross-section for production of an isolated lepton and missing transverse momentum is due to virtual W exchange in the t-channel. This process generates events with a lepton–neutrino transverse mass $M_T^{\ell\nu}$ which can be low.

The above processes are studied quantitatively with a Monte-Carlo program EPVEC [6] interfaced to the JETSET hadronization model [8] and a full simulation of the H1 detector response.

The acceptance of the event selection procedure described in section 2.2 combined with isolation cuts $D_{jet} > 0.5$ and $D_{track} > 0.5$, is shown in figure 7 as function of P_T^X for the electron and muon channels separately. The overall acceptance is 40% for the electron channel and 12% for the muon channel. The quoted acceptance include trigger efficiencies. The difference is due to the dominance of the cross-section at low P_T^X values, for which little energy is seen in the calorimeters in the muon channel. At high P_T^X ($P_T^X > 40$ GeV) the muon channel acceptance reaches a plateau of 60%. The lower electron channel acceptance in this region is due to the fact that depending on the electron decay azimuthal direction, the electron energy deposits in the LAr calorimeter may partly balance those of the hadronic system, resulting in a calorimetric missing transverse momentum P_T^{calo} lower than the threshold of 25 GeV.

The cascade decay $W \to \tau \to$ e, μ gives $\sim 20\%$ contribution in the total number of expected events.

3.2 Comparison of data to W production

The interpretation of all five events as W production is kinematically acceptable. Figure 8 shows (dots), for a luminosity a factor 500 higher than in the data, the expected distribution of W events in the (P_T^X,$M_T^{\ell\nu}$) variables . The corresponding values measured for the five events are indicated by the ellipse contours. As discussed above, the W events accumulate at large $M_T^{\ell\nu}$ values and low values of P_T^X. The muon events are accepted only when produced with a sizeable hadronic recoil transverse momentum.

In this plot the MUON-4 event shows up with a large error on $M_T^{\ell\nu}$ because of the poor determination of the isolated muon transverse momentum.

In the e^- event and the MUON-3 event the hadronic recoil system has a relatively small transverse momentum and the $M_T^{\ell\nu}$ values show up in the Jacobian peak close to the W mass. For the MUON-3 event a scattered positron is observed in the detector. Identifying this particle with the scattered positron allows the invariant mass of the muon-neutrino system to be calculated. The result is $M_{\mu\nu} = 83^{+15}_{-10}$ GeV in good agreement with the W mass.

In contrast, the MUON-1, MUON-2 and MUON-4 events show high P_T^X values together with low $M_T^{\ell\nu}$ values for MUON-1 and MUON-2.

Tables 2a) and b) compare the observed and expected numbers of events in several regions of phase space, defined by various P_T^X and $M_T^{\ell\nu}$ cuts, for the electron and muon channels respectively. In total 1.34 events and 0.41 events are expected in the $e^\pm$ and $\mu^\pm$ channels respectively.

The error estimate on the predicted number of events includes:

- the experimental error taking into account uncertainties on the calorimetric energy scale and the measured luminosity.
- QCD scale uncertainty. This is estimated by varying the QCD scale at which W's are produced from 100 GeV^2 to 10000 GeV^2.

In a region of phase space defined by $P_T^X > 40\,\mathrm{GeV}$ and $M_T^{\ell\nu} < 30\,\mathrm{GeV}$ one observes 2 muon events compared to an expectation of 0.02 ± 0.003 events.

It should be emphasized that the cross-sections from [6] used in the predictions are based on leading order computations. It is presently not known whether higher order QCD terms may significantly change the prediction, especially as regards the P_T^X spectrum.

a) electron	$M_T^{\ell\nu} < \infty$	$M_T^{\ell\nu} < 60\ GeV$	$M_T^{\ell\nu} < 30\ GeV$
$P_T^X > 0$GeV	$1\ /\ 1.34 \pm 0.05 \pm 0.20$	$0\ /\ 0.33 \pm 0.01 \pm 0.05$	$0\ /\ 0.04 \pm 0.003 \pm 0.006$
$P_T^X > 20$GeV	$0\ /\ 0.40 \pm 0.05 \pm 0.06$	$0\ /\ 0.15 \pm 0.005 \pm 0.02$	$0\ /\ 0.04 \pm 0.003 \pm 0.006$
$P_T^X > 40$GeV	$0\ /\ 0.11 \pm 0.02 \pm 0.02$	$0\ /\ 0.05 \pm 0.005 \pm 0.006$	$0\ /\ 0.02 \pm 0.002 \pm 0.003$
b) muon	$M_T^{\ell\nu} < \infty$	$M_T^{\ell\nu} < 60\ GeV$	$M_T^{\ell\nu} < 30\ GeV$
$P_T^X > 20$GeV	$4\ /\ 0.41 \pm 0.02 \pm 0.06$	$2\ /\ 0.17 \pm 0.01 \pm 0.03$	$2\ /\ 0.06 \pm 0.002 \pm 0.01$
$P_T^X > 40$GeV	$3\ /\ 0.13 \pm 0.02 \pm 0.02$	$2\ /\ 0.05 \pm 0.005 \pm 0.008$	$2\ /\ 0.02 \pm 0.001 \pm 0.003$

Table 2: Observed (numerator) over predicted (denominator) number of events as function of the P_T^X and $M_T^{\ell\nu}$ cuts: a) electron channel b) muon channel. The prediction is for W production with leptonic decay. The first error is the experimental error and the second one is due to the QCD scale uncertainty.

3.3 Other physics processes

In the following we discuss other sources (for details see [1]) which could lead to events with isolated leptons and a P_T imbalance.

- Production of a heavy quark pair (charm or bottom) with the subsequent semileptonic decay of one of the quarks. These processes have been simulated with high statistics using the PYTHIA generator [9], resulting in an accepted cross section of less than 0.1 fb. The expected event rate from this process is thus negligible. A data set corresponding to a luminosity of 500 pb^{-1}has been fully simulated and analysed with no event surviving the selection.

- Production of τ pairs has been studied using the LPAIR generator [10]. A $\tau^+\tau^-$ event, where one τ decays hadronically and the other leptonically, could show the topology of the observed events. From a sample corresponding to 9 fb^{-1} generated with τ transverse momenta above 15 GeV, only 2% have a missing transverse momentum above 25 GeV. After all analysis cuts, the expected number of events in the electron and muon channels are 0.03 and 0.02 respectively.

  The tau hadronic jets have low multiplicity and low mass. The probability that a hadronic tau jet has a reconstructed mass greater than 5 GeV is low (5%). In addition, the track multiplicity in the observed events is high (> 5) making the τ pair production an unlike explanation of the observed events.

The event rate from the sources considered above sums to less than 0.05 events.

4 Summary

In positron proton scattering at HERA a sample of 336 events has been selected requiring a significant imbalance in transverse momentum. While the majority of the events have topologies as expected from deep inelastic charged current scattering processes, five events show the prominant signature of an isolated high P_T lepton. Within the standard model the only source of significant rate predicted for this kind of topology is the production of W. Two of the five events are found in a region of phase space likely to be populated by $W^{\pm}$ production.

Acknowledgements

We are grateful to the HERA machine group whose outstanding efforts have made and continue to make this experiment possible. We thank the engineers and technicians for their work in constructing and now maintaining the H1 detector, our funding agencies for financial support, the DESY technical staff for continual assistance, and the DESY directorate for the hospitality which they extend to the non-DESY members of the collaboration.

References

[1] H1 Collaboration, DESY preprint DESY 94-248.

[2] H1 Collaboration, S. Aid et al.,Z.Phys.C71 (1996) 211.

[3] H1 Collaboration, Z.Phys.C67 (1995) 565, Phys.Lett. B379 (1996) 319.

[4] H1 Collaboration, I. Abt et al., Nucl. Instr. and Meth. A386 (1997) 310 and 348.

[5] H1 Calorimeter Group, B. Andrieu et al., Nucl. Instr. and Meth. A336 (1993) 460.

[6] U.Baur, J.A.M. Vermaseren, D. Zeppenfeld, Nucl. Phys. B375 (1992) 3.

[7] E. Boos, private communication.

[8] T. Sjöstrand, Comp. Phys. Com. 39 (1986) 347.

[9] T. Sjöstrand, CERN-TH-6488 (1992),Comp. Phys. Comm 82 (1994) 74.

[10] S.Baranov et al., Proc. of Workshop Physics at HERA, W. Büchmüller and G. Ingelman (Editors), (October 1991,DESY-Hamburg) Vol. 3, p. 1478; J.A.M. Vermaseren, Nucl. Phys. B229 (1983) 347.

Figures

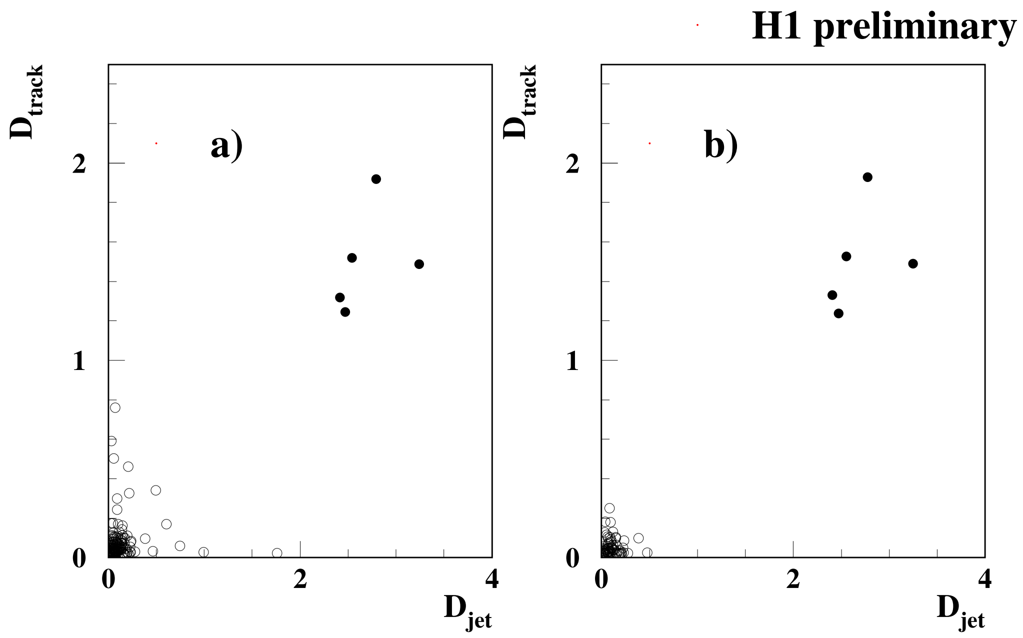

Figure 1: Correlation between the distances D_{jet} and D_{track} of high energy tracks to its closest hadronic jet and closest track (see text): a) All tracks with transverse momenta above 10 GeV in the CC event sample; b) Tracks matching in addition the electron or muon identification criteria.

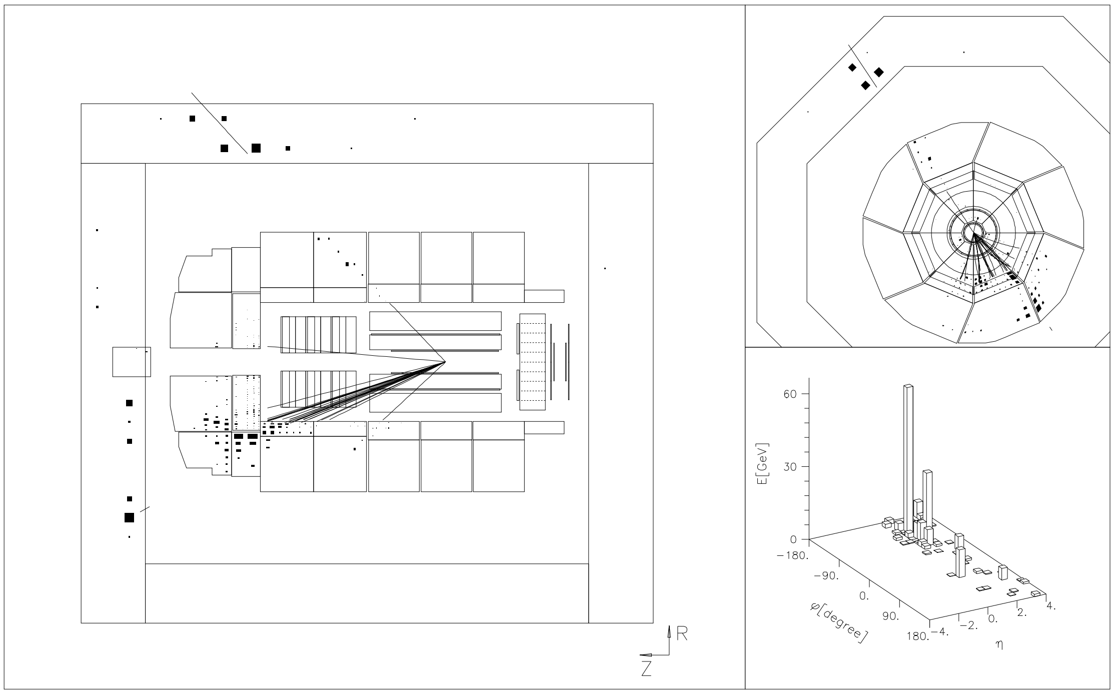

Figure 2: Display of the μ^+ event (MUON-1). Shown are a side view (left) and a transverse view of the event. The "Legoplot" shows the observed calorimetric energy depositions in the $\eta - \phi$ plane.

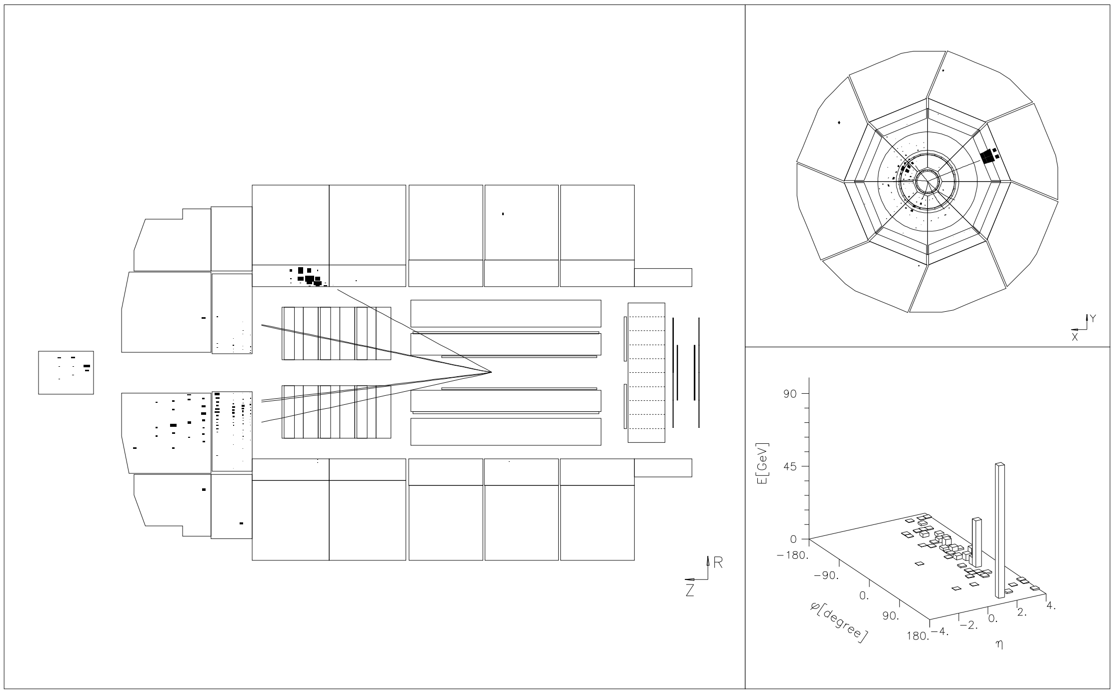

Figure 3: Display of the e^- event (ELECTRON)

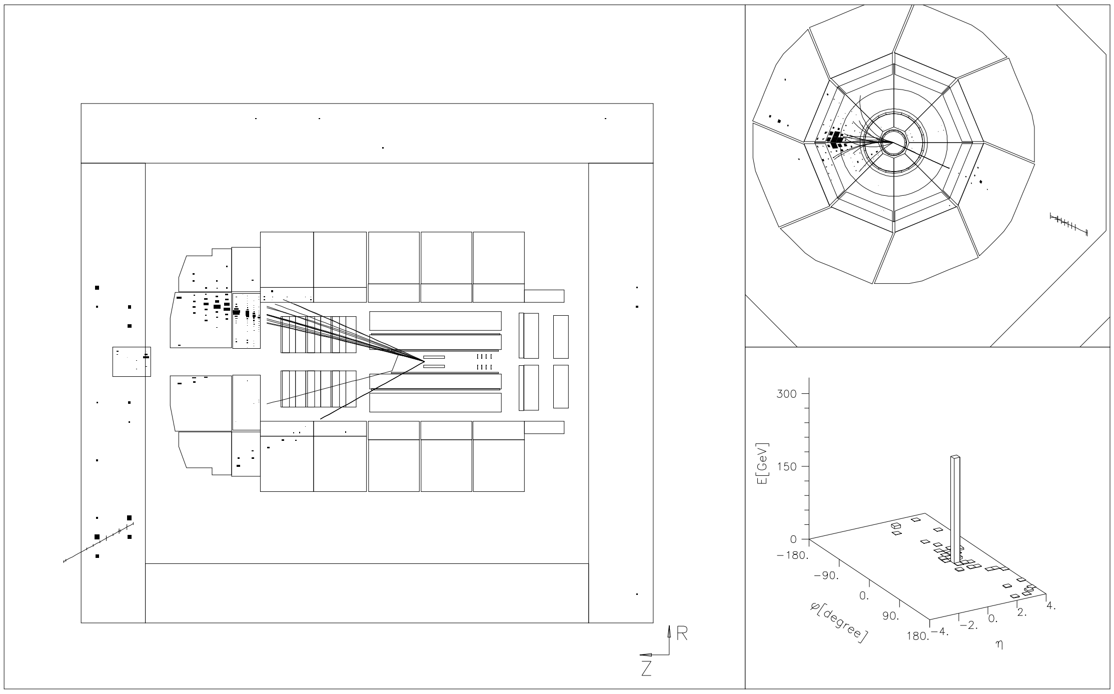

Figure 4: Display of the μ^+ event (MUON-2)

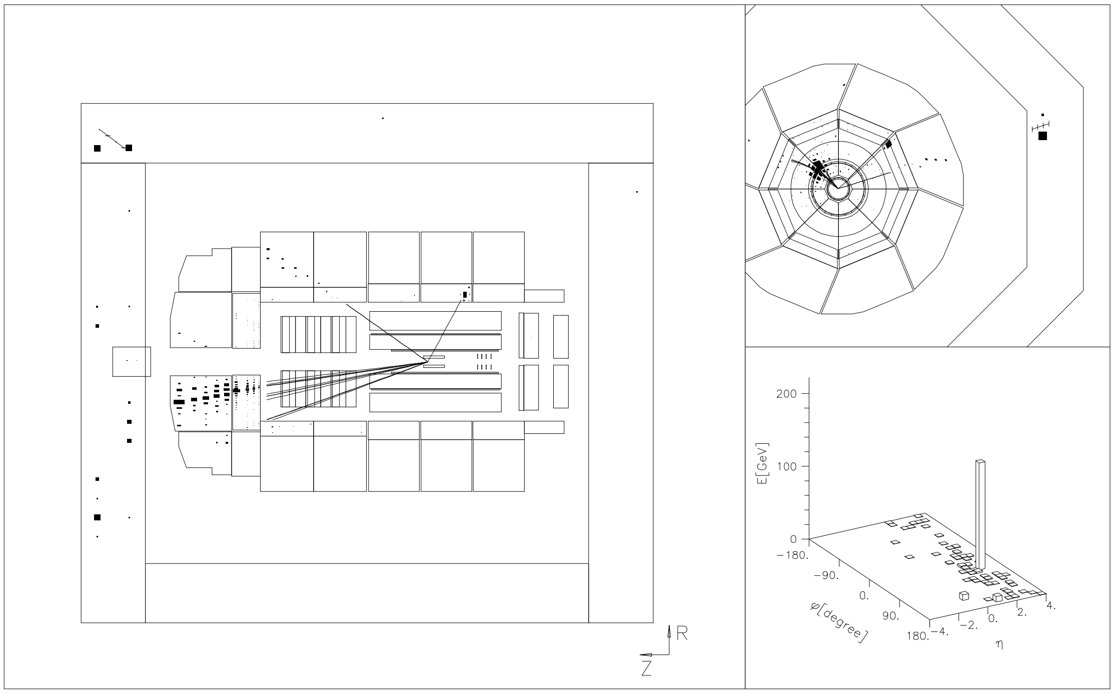

Figure 5: Display of the μ^- event (MUON-3). In this event an additional positron is visible.

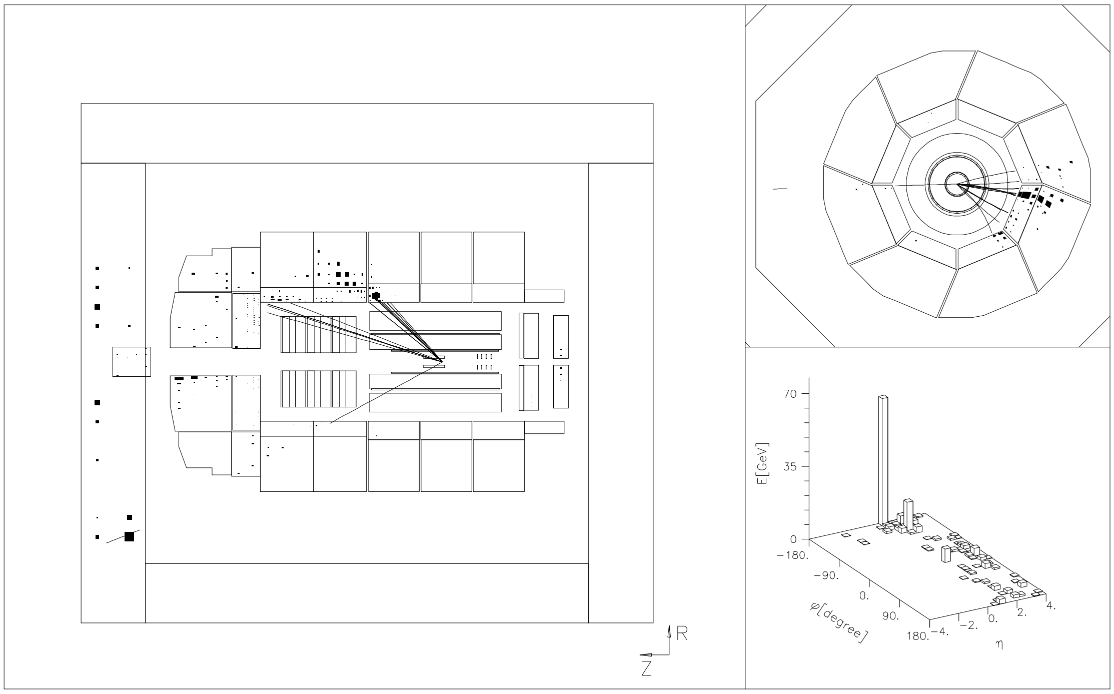

Figure 6: Display of the μ^- event (MUON-4)

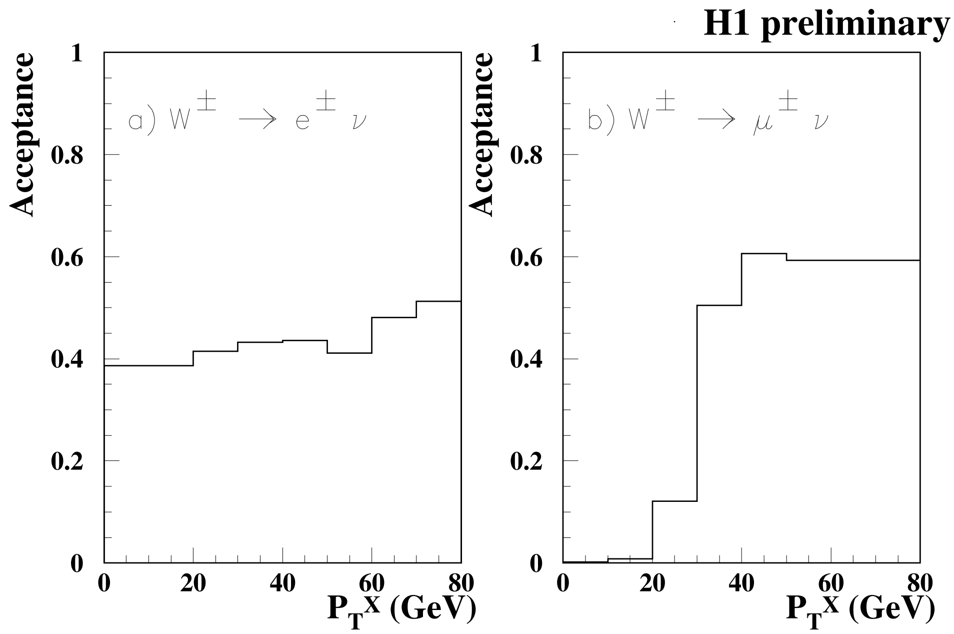

Figure 7: Acceptance of the event selection as function of the hadronic recoil transverse momentum P_T^X : a) electron channel; b) muon channel.

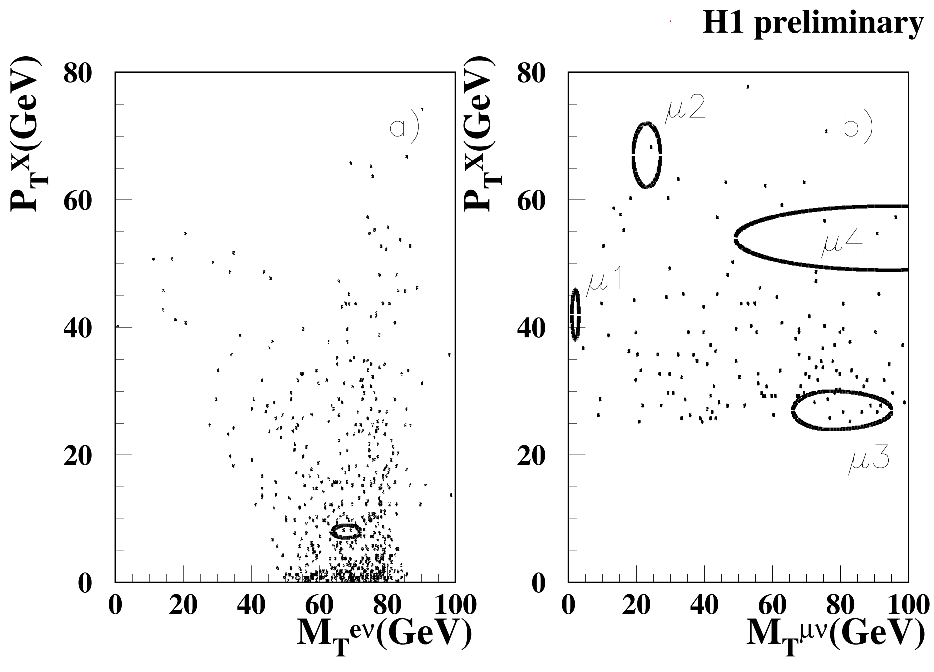

Figure 8: Distribution of the five events (ellipses) in P_T^X and $M_T^{l\nu}$: a) electron channel; b) muon channel. The ellipse contours correspond to the 1-sigma uncertainty on the measured parameters of each event. The points show the standard model expectation for W production for an accumulated luminosity a factor 500 higher than in the data.